ngVLA Memo no. 131

Self-calibration of ngVLA simulated observation

Viral Parekh
vparekh@nrao.edu
National Radio Astronomy Observatory, Socorro, NM

June 10, 2025

Abstract

In this memo, we studied the effects of static and time-varying phase errors on ngVLA simulation to study dynamic range (DR). We used the deep field continuum model comprising 6000 point sources (clean components) over a 6-arcmin field. We simulated this model with ngVLA Band 1 (at the center frequency of 2 GHz) and then added four (±5,±10,±25 and ±40deg) uniformly distributed phase errors over time intervals of 5, 10, and 15 mins (of total observation time of 30 mins) to each antenna. These time-dependent phase errors smear the image and reduce the image DR. After the first imaging, we performed four successive phase-only self-calibration in CASA. We found that self-calibration can improve the DR by factor $\sim$ 4x for large phase errors. For small phase errors, three rounds are enough to achieve sufficient DR. Static phase errors are constant, and time-invariant offsets at each antenna introduce fixed distortions in visibilities without significantly degrading DR. We also found after self-calibration the residual phase error constrain within ±2°.

1 Introduction

The next-generation VLA (ngVLA) is an advanced interferometric array currently being under construction. The future ngVLA will improve the sensitivity and spatial resolution of the current VLA (VLA) and ALMA telescopes by more than an order of magnitude. The ngVLA is designed to observe the sky at radio frequencies range of 1.2 GHz (21 cm or L-band) to 116 GHz (2.6 mm), constructed on the legacy of the major VLA, ALMA, and the VLBA instruments. The ngVLA will be a fantastic telescope for observing broadband continuum emission of non-thermal radio sources. However, this broadband imaging will bring numerous challenges, particularly at low frequencies. All current radio observations (particularly at low frequencies below L-band) suffer from phase corruption due to atmosphere, RFI, delay, pointing errors, and unknown calibration errors (both direction-independent and direction-dependent) associated with large field of view and broad bandwidth. In order to achieve a high-dynamic range (HDR) and detect fainter radio sources, one has to understand these errors and need to remove them from the data.

2 ngVLA simulation

Here we performed ngVLA simulation using the main antenna configurations (214 telescopes with core, spiral, and mid baselines) for 30 mins in total time with 60 sec integration time. In this simulation, we want to corrupt the visibilities by adding constant phase errors as well as time-varying phase errors. We also want to apply self-calibration to this corrupted data to study how we can remove the phase errors from the data and estimate the DR (peak/rms). In this simulation, we used the CASA 6.6 v. We employed CASA's `simobserve` task to simulate the sky model and generate the measurement set. We used the bandwidth of 100 MHz with a single channel to keep the small data volume. For this simulation, we used ngVLA Band 1, center frequency 2 GHz. We did not add any noise (thermal) to the visibility so our simulation is noise-free.

2.1 Model

In our simulation, we used the deep field imaging model from the ngVLA simulation model repository. The model is comprised of 6000 compact point sources over a 6-arcmin field. This model is derived using an S-cubed radio sky simulator. The given model is at a frequency of 8 GHz and contains a total flux of $\sim$ 8mJy. The phase-centre of the model is RA=0.0deg and Dec=30deg. In order to use this model for ngVLA Band 1, we simply changed the header parameter (of the Model) `'CRVAL3'` to 2000e6 Hz. We have not converted the flux values of model sources from 8 GHz to 2 GHz because studying source properties is not our goal in this simulation. In this model, the clean components are in the range of 0.5 nJy to 4mJy. Based on the frequency, we changed the resolution of the input model (`CDELT1` and `CDELT2`) such that the ngVLA main configuration's longest antennas can sample the model visibilities.

2.2 Visibility corruption

Phases of the radio interferometer signals are corrupted by atmosphere, imperfect instruments, RFI, calibration error, etc. These phase errors can degrade the DR and quality of the final radio image of the target source. Here we simulate the constant and time-varying antenna-based uniformly distributed random phase errors and add them to the simulated measurement set. We added $\pm5^\circ$, $\pm10^\circ$, $\pm25^\circ$ and $\pm40^\circ$ phase errors for every 5, 10, and 15 mins. This will help to estimate how the ngVLA DR, for a given model, will be affected by the phase errors.

2.3 Imaging and Self-calibration

These phase variations in the data can be mitigated by several techniques, for example, self-calibration. After adding the phase errors, we performed the imaging and self-calibration using `tclean` and `gaincal` tasks. In tclean, we used the following parameters - imsize=720, cellsize=0.22asec, weighting='briggs', robust=0, deconvolver='hogbom', loopgain=0.1, and niter=10000. After imaging, we performed four rounds of phase-only self-calibration with solution intervals of 15 min, 10 min, 5 min, and int (60 sec). With ngVLA main configuration (B_{max} = 1068 km) we obtained a beam size of $0.74'' \times 0.72''$ for our images (for weighting robust zero).

3 Result

In this section we show our simulation results. Figure 1 shows the imaging and selfcal maps after adding ±5° for every 5-minute time interval to our simulated measurement set. We also listed rms measurements for each of the maps. There is a bright source at RA=359.98° and Dec=30.01° located at ∼ 1.4' away from the phase-centre towards NW direction causing more errors around it and degrading rms with increasing phase errors. This bright source dominates the sidelobe levels and distorts the point spread function (PSF) with increasing phase errors. We can reduce these sidelobes in a self-calibration as shown in Figures 1 to 4.

Table 1 lists the DR in our simulation before (Image1) and after self-calibration (Image_SC). Figures 2, 3, and 4 show the maps for ±10°, ±25° and ±40° phase errors for 10 min and 15 min, respectively. Figure 5 shows the gain solutions plot for Phase vs Time. We can see residual phase errors, after self-calibration, for each antenna, constrain within ±2°.

Table 1: Dynamic Range (DR) values for different phase errors and time intervals.

Image Type	±5°	±10°	±25°	±40°
Time interval: 5min				
Image1	4500	2739	1214	740
Image_SC	4800	3000	1380	814
Image_SC2	5161	3293	1550	932
Image_SC3	7361	6536	4052	2362
Image_SC4	7641	7416	5420	3000
Time interval: 10min				
Image1	4763	2914	1224	804
Image_SC	5328	3295	1477	939
Image_SC2	5761	3848	1855	1210
Image_SC3	7505	7131	4561	2630
Image_SC4	7638	7456	5200	2915
Time interval: 15min				
Image1	4817	3164	1374	843
Image_SC	5601	3845	1732	1069
Image_SC2	6947	6184	3680	2266
Image_SC3	7487	7179	5124	3047
Image_SC4	7556	7329	5522	3251
Time interval: 30min				
Image1	7640	7640	7640	7640
Image_SC	7650	7650	7650	7650
Image_SC2	7265	7265	7265	7265
Image_SC3	7588	7588	7588	7588
Image_SC4	7594	7594	7594	7594

4 Discussion

Based on the self-calibration results, we see the rms and DR improvements after the successive phase-only selfcal rounds for time-varying phase errors added to the simulated ngVLA observation. For larger phase errors of ±25° and ±40° selfcal can improve ∼ 4-5 times DR with smaller solution intervals which captures residual phase errors effectively. For smaller

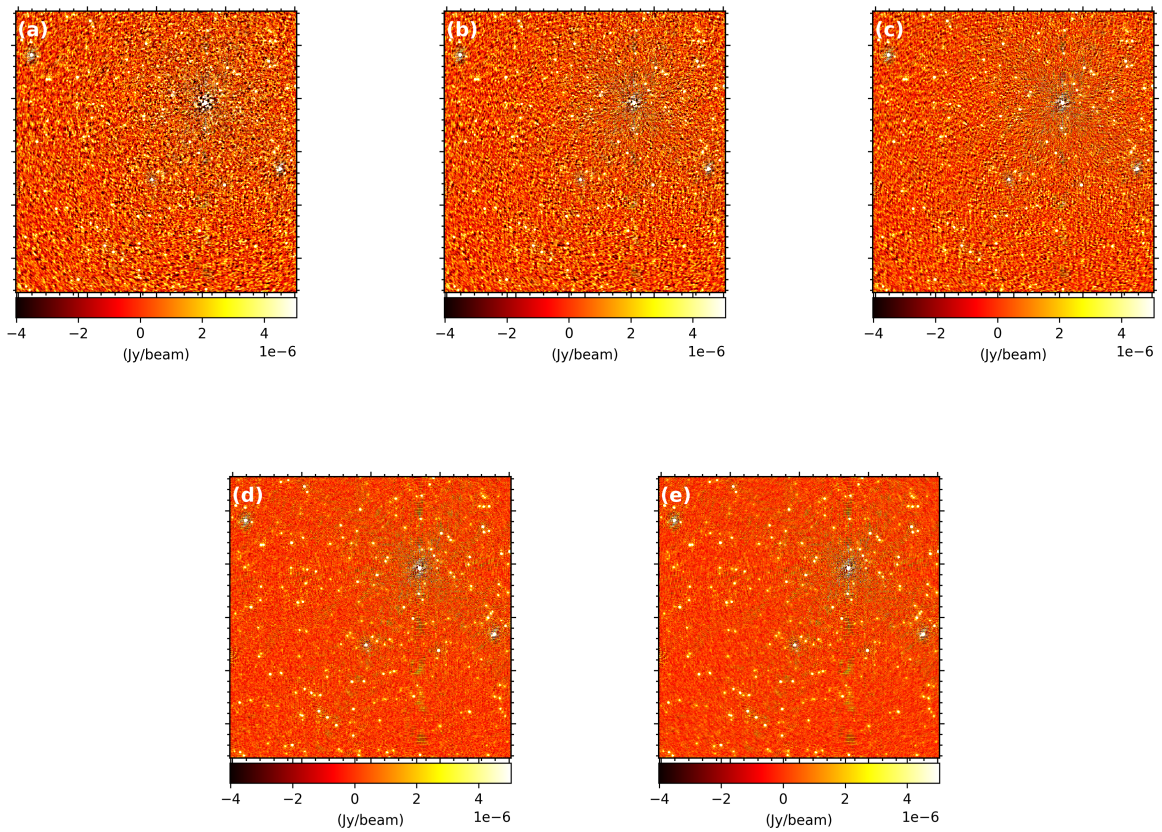

Figure 1: (a) ±5° phase error added for every 5 mins (rms=1.87 μJy beam^{-1}). (b) After selfcal round 1 (solint=15min, rms=1.76 μJy beam^{-1}). (c) After selfcal round 2 (solint=10min, rms=1.64 μJy beam^{-1}). (d) After selfcal round 3 (solint=5min, rms=1.15 μJy beam^{-1}). (d) After selfcal round 4 (solint=int, rms=1.11 μJy beam^{-1}).

phase error (±5°), three rounds of selfcal is sufficient. Static phase errors are constant phase offsets (same values as time-varying offsets) applied to each antenna throughout the entire observation (30 min total observation time). These phase errors introduce a fixed distortion in the visibilities but do not vary with time, so they preserve coherence and typically do not degrade DR significantly unless they are large. As discussed in ngVLA memo 114, theoretically, the expected DR value for constant phase errors is DR$_{exp}$=$\frac{N_{ant}}{\sqrt{2}\times\sigma}$, where N$_{ant}$ is number of antennas in simulation (214) and σ is RMS phase error in radian (Perley 1998). In our worst case of phase error of 40°, then DR$_{exp}$=217. After self-calibration, the phase error goes down to $\leq$ 2° so DR$_{exp}$ $\sim$ 4300. If phase errors are random in time, the predicted DR$_{exp}$ will be increase by factor of 5 ($\sqrt{timestamps}$=$\sqrt{1800/60}$). This value is too large compared to our DR measurements from the simulation. However, there are a few factors that need to be taken an account here. The definition of DR$_{exp}$ described by Perley (1998) assumes Natural weighting, while in our simulation we applied robust weighting. This will decrease the number of antennas away from the dense core. Robust weighting is similar to the Uniform weighting and all antennas do not have equal weights as compared to Natural weighting. The other factor is the definition of DR. For deep field observations, it is important to account for the contribution of sidelobe noise from multiple bright sources, both within and outside the primary beam. For deep and sensitive wide-band observations, estimating the true rms background noise becomes difficult in the presence of numerous point sources. Therefore, the expected DR is only an approximation, and additional imaging-related errors may be

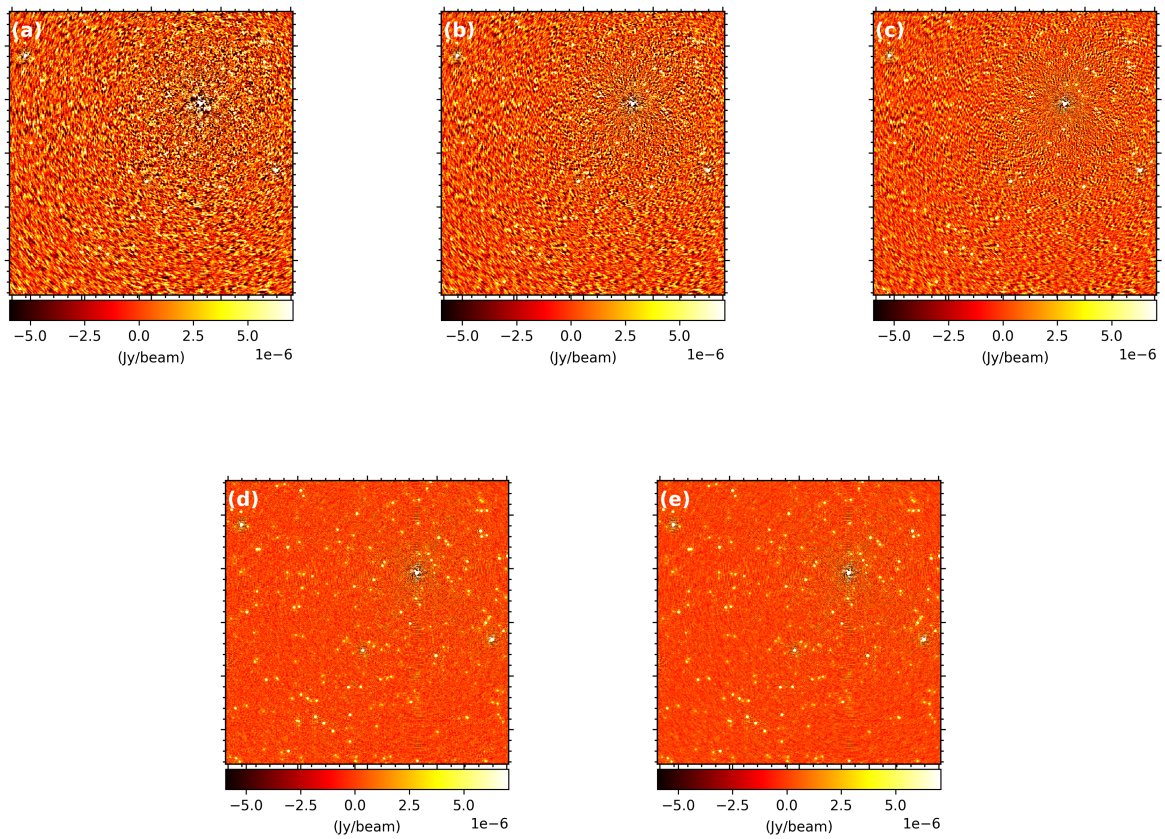

Figure 2: (a) ±10° phase error added for every 10 mins (rms=2.88 μJy beam^{-1}). (b) After selfcal round 1 (solint=15min, rms=2.55 μJy beam^{-1}). (c) After selfcal round 2 (solint=10min, rms=2.19 μJy beam^{-1}). (d) After selfcal round 3 (solint=5min, rms=1.18 μJy beam^{-1}). (d) After selfcal round 4 (solint=int, rms=1.13 μJy beam^{-1}).

present in the simulated images beyond just phase errors.

5 Future plan

We want to understand different calibration-related errors and how effectively we can solve them to improve the DR for future ngVLA. In this memo, we only simulated time-varying phase errors. Next, we will study time and frequency-dependent phase and amplitude errors and how they affect the ngVLA data.

Acknowledgement

VP acknowledges Kumar G. and Carilli C. for the fruitful discussion on ngVLA simulation.

References

(1) ngVLA memo 35
(2) ngVLA memo 114
(3) Synthesis Imaging in Radio Astronomy II, 1998

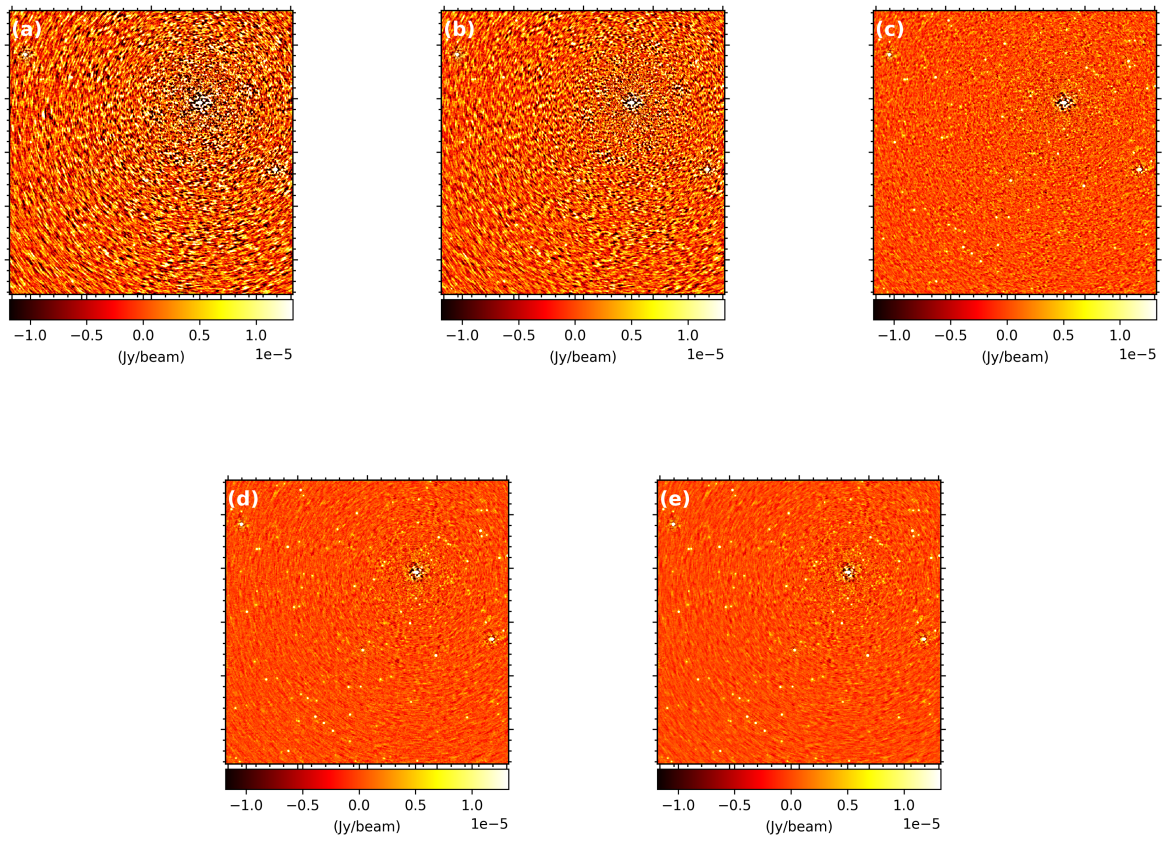

Figure 3: (a) ±25° phase error added for every 15 mins (rms=5.95 μJy beam^{-1}). (b) After selfcal round 1 (solint=15min, rms=4.79 μJy beam^{-1}). (c) After selfcal round 2 (solint=10min, rms=2.29 μJy beam^{-1}). (d) After selfcal round 3 (solint=5min, rms=1.65 μJy beam^{-1}). (d) After selfcal round 4 (solint=int, rms=1.54 μJy beam^{-1}).

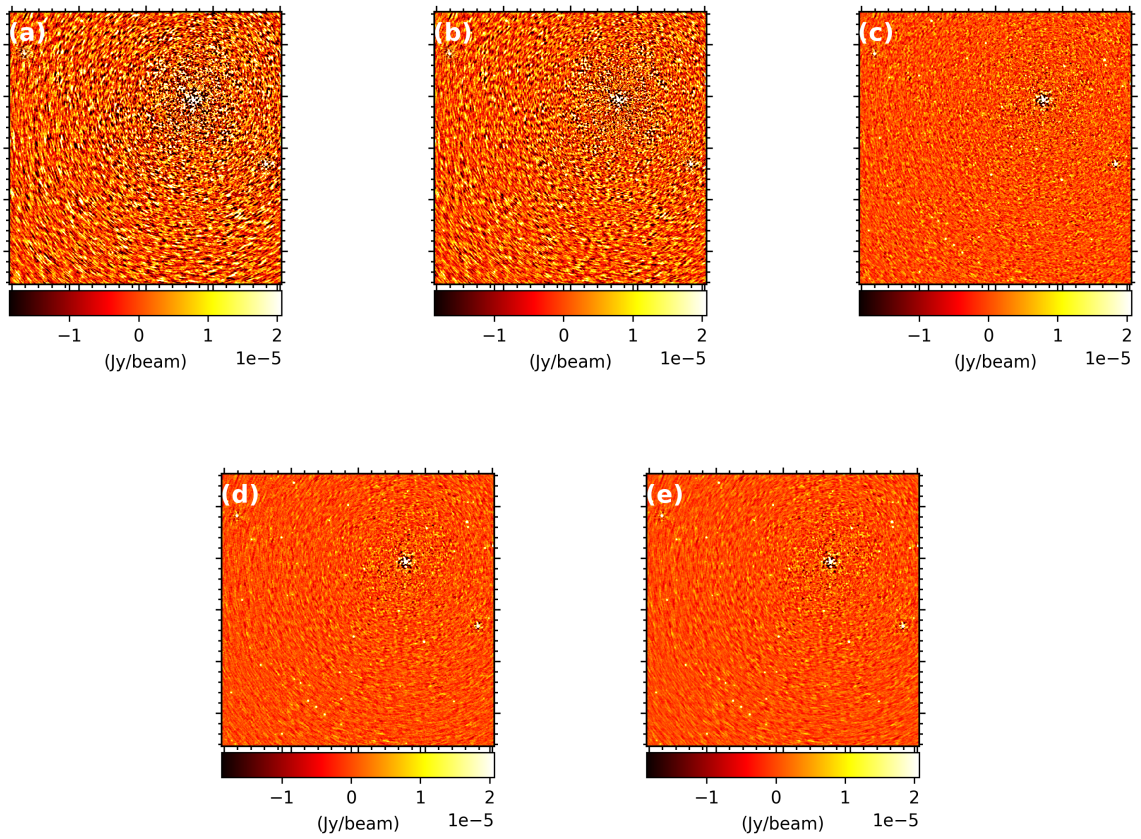

Figure 4: (a) $\pm 40^{\circ}$ phase error added for every 15 mins (rms=9.25 μJy beam^{-1}). (b) After selfcal round 1 (solint=15min, rms=7.56 μJy beam^{-1}). (c) After selfcal round 2 (solint=10min, rms=3.72 μJy beam^{-1}). (d) After selfcal round 3 (solint=5min, rms=2.80 μJy beam^{-1}). (d) After selfcal round 4 (solint=int, rms=2.62 μJy beam^{-1}).

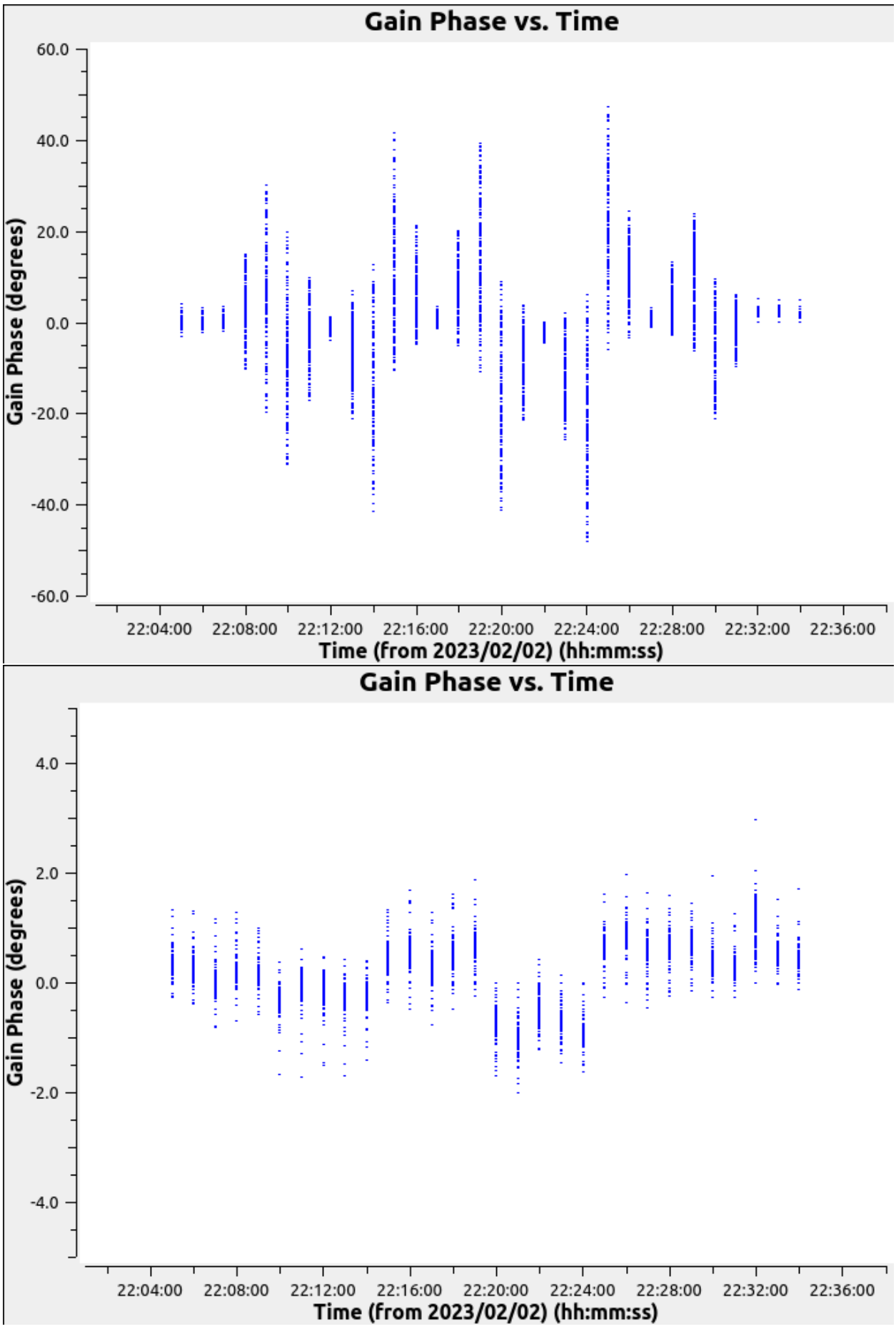

Figure 5: Gain solution plots of Phase vs Time. **Top** plot shows the ±40° phase fluctuations for every 5 min time interval for total 1800s observation length. **Bottom** plot shows phase stability after self-calibration.